Polyhedron 51 (2013) 46–53

Contents lists available at SciVerse ScienceDirect

Polyhedron

journal homepage: www.elsevier.com/locate/poly

Activation of ortho C–H bond by nickel(II) acetate or sodium tetrachloropalladate(II) in naphthyl imino derivatives of azobenzene

Debprasad Patra [a,b], Poulami Pattanayak [a], Jahar Lal Pratihar [a,c], Surajit Chattopadhyay [a,*]

[a] Department of Chemistry, University of Kalyani, Kalyani 741235, India
[b] Department of Chemistry, East Calcutta Girls' College, Kolkata 700089, India
[c] Department of Chemistry, Kandi Raj College, Murshidabad 742137, India

ARTICLE INFO

Article history:
Received 5 November 2012
Accepted 15 December 2012
Available online 23 December 2012

Keywords:
1-{[2-(Arylazo)phenyl]iminomethyl}-2-naphthol
Orthometallation
O-insertion
Luminescent property

ABSTRACT

The reactions of 1-{[2-(arylazo)phenyl]iminomethyl}-2-naphthol, H_2L_{nap} [where H represents the dissociable proton upon complexation and aryl groups of H_2L_{nap} are phenyl for $H_2L^{1}{}_{nap}$; *p*-methyl phenyl for $H_2L^{2}{}_{nap}$ and *p*-chloro phenyl for $H_2L^{3}{}_{nap}$] with nickel acetate tetra hydrate or disodium tetrachloropalladate in methanol afforded M–C(aryl) bonded species of composition $[M(L_{nap})]$ (M = Ni(II) and Pd (II)). The dinegative $(L_{nap})^{2-}$ ligands bind the Ni(II) or Pd(II) in tetradentate (C, N, N, O) fashion in distorted square planar geometry. Ligands and complexes were characterized by spectroscopic methods. The X-ray structures of $H_2L^{1}{}_{nap}$, $[Ni(L^{1}{}_{nap})]$ and $[Pd(L^{1}{}_{nap})]$ were determined to authenticate the characterization. Reactions with metachloroperbenzoic acid (mCPBA), TBHP and hydrogen peroxide leading to oxygen insertion into the M-C bond have been examined. Luminescent properties of ligands and complexes have been reported.

1. Introduction

Catalytic conversion of C–H bonds into C–C, C–N, C–O and C–halogen bonds by means of metal assisted C–H activation is one of the important areas in current chemical research to search for suitable catalyst [1,2]. Studies are ongoing to develop appropriate low cost alternative catalysts, with comparatively cheap and abundant metal ions, that are capable of C–H activation. Recently, first $[Ni(COD)_2]$ catalyzed chemical transformation via activation of ortho C–H bond has been reported with a mention that there was no such example though chelation assisted orthonickelation of azobenzene was achieved by treating with $[Ni(Cp)_2]$ quite a long ago [3]. Facile activation of ortho C–H bond and stoichiometric C–O bond formation under ordinary condition using the common reagent nickel acetate has been reported [4]. Although, the reaction was not catalytic but provided the clue toward use of commonly available nickel compound as catalyst for the transformations involving ortho C–H activation. Thus, having realized the importance, we were encouraged to study the hydroxylation of different organic substrates through chelation assisted activation of ortho C–H bond by nickel acetate. Comparison of the reactivity of M–C bond between M = Ni(II) and M = Pd(II) is also relevant to realize the advantages.

This work stems from our interest on synthesis of metalloazosalophens **1** [4–6]. As reported earlier, synthesis of metalloazosalophens can be carried out in two ways – first, synthesis of M–C (aryl) bonded complex (ortho C–H cleavage) using nickel acetate or sodium tetrachloropalladate followed by oxygen insertion into M–C bond i.e. C–O bond formation (Scheme 1). This procedure was shown to be applicable for the compound H_2L_{sal}, **2** [4,6]. Secondly, Synthesis of authentic azosalophen ligand, H_2OL_{sal}, **3**, via nickel assisted hydroxylation followed by complexation with appropriate transition metal substrates (Scheme 2) [4–8].

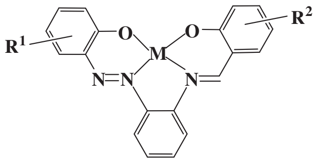

1

Synthesis of new analogs of H_2L_{sal}, **2** and its conversion to an analog of H_2OL_{sal}, **3**, using nickel acetate or sodium tetrachloropalladate were contemplated to illustrate that the C–H activation by nickel acetate or sodium tetrachloropalladate can also take place in the analogs of H_2L_{sal}. As a sequel, the new analog, containing naphthyl group, H_2L_{nap}, shown in **4**, have been used for the present purpose [9]. Incorporation of naphthyl group within the ligand

---

* Corresponding author. Tel.: +91 33 25828750; fax: +91 33 25828282.
E-mail address: scha8@rediffmail.com (S. Chattopadhyay).

0277-5387/$ - see front matter © 2012 Elsevier Ltd. All rights reserved.
http://dx.doi.org/10.1016/j.poly.2012.12.011

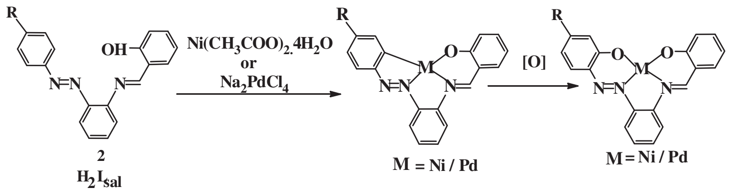

Scheme 1.

backbone was conceived with the expectation that the complexes prepared with **4** might exhibit interesting absorption and/or emission properties due to the inherent luminescent property of naphthyl group [9–19].

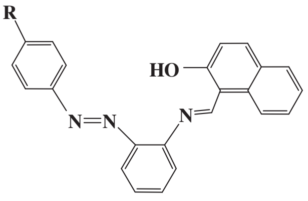

4

Herein we have described the orthometallation in H_2L_{nap} by treating with $Ni(CH_3COO)_2{\cdot}4H_2O$ or Na_2PdCl_4. The products were characterized by UV–Vis, IR and ^1H NMR spectroscopic data. The X-ray structures of $H_2L^1_{nap}$ and newly synthesized Ni(II) and Pd(II) orthometallated complexes have been determined for unequivocal characterization. The reactions of new Ni–C and Pd–C bonded complexes with peroxo compounds, leading to C–O bond formation, have been reported. Emission properties of the ligands and corresponding complexes have been compared and delineated in this paper.

2. Results and discussion

2.1. Syntheses

Reaction of 1-{[2-(arylazo)phenyl]iminomethyl}-2-naphthol, H_2L_{nap}, with $Ni(OAc)_2{\cdot}4H_2O$ in refluxing methanol afforded green precipitate which upon purification by washing with methanol gave pure complexes of Ni(II) of composition $[Ni(L^1_{nap})]$, **5**. Similarly the reaction of Na_2PdCl_4 with H_2L_{nap} in stirring methanol afforded brown complexes of Pd(II) of composition $(L_{nap})Pd$, **6**. The synthetic reactions are shown in Eq. (1) below:

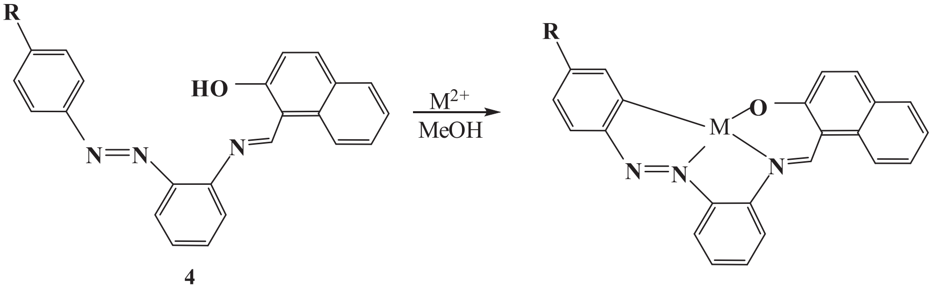

4
H_2L_{nap}

M= Ni^{2+}, $[Ni(L_{nap})]$, **5** and M= Pd^{2+}, $[Pd(L_{nap})]$,**6**

		R
$H_2L^1_{nap}$	**4a**	H
$H_2L^2_{nap}$	**4b**	CH_3
$H_2L^3_{nap}$	**4c**	Cl
$[Ni(L^1_{nap})]$	**5a**	H
$[Ni(L^2_{nap})]$	**5b**	CH_3
$[Ni(L^3_{nap})]$	**5c**	Cl
$[Pd(L^1_{nap})]$	**6a**	H
$[Pd(L^2_{nap})]$	**6b**	CH_3
$[Pd(L^3_{nap})]$	**6c**	Cl

(1)

2.2. Reactions with oxidants

The newly synthesized orthometallated complexes $[Ni(L^1_{nap})]$, **5**, and $[Pd(L^1_{nap})]$, **6**, transformed into the oxygenated products

[Ni(OL$^1{}_{nap}$)], **7**, and [Pd(OL$^1{}_{nap}$)], **8**, respectively upon reaction with *meta* chloroperbenzoic acid (*m*CPBA) as given in Eqs. (2) and (3).

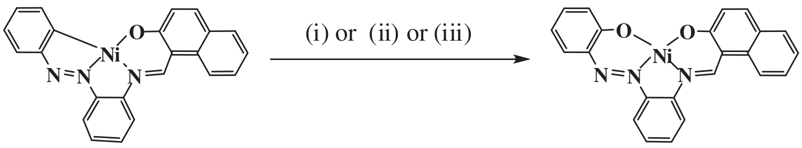

[Ni(L$^1{}_{nap}$)], **5** [Ni(OL$^1{}_{nap}$)], **7** (2)

(i) *m*-CPBA, CH_2Cl_2 ; (ii) Aqueous H_2O_2, CH_2Cl_2 ; (iii) TBHP, CH_2Cl_2 or ^{t}BuOH

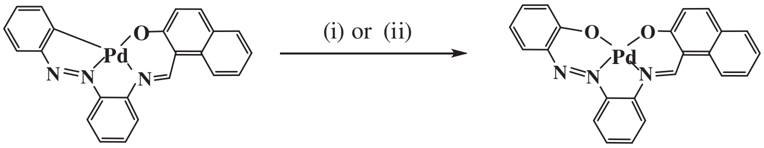

[Pd(L$^1{}_{nap}$)], **6** [Pd(OL$^1{}_{nap}$)], **8** (3)

(i) *m*-CPBA, CH_2Cl_2 ; (ii) TBHP, $VO(acac)_2$, CH_2Cl_2 or ^{t}BuOH

Although the oxygen insertion was relatively slower for [Pd(L$^1{}_{nap}$)] but it was very fast in the case of [Ni(L$^1{}_{nap}$)]. Gradual change in absorption spectrum with time could be measured spectrophotometrically for [Pd(L$^1{}_{nap}$)] adding quantitative amount of *m*CPBA (Fig. 1) in dichloromethane solution.

Moreover, [Ni(L$^1{}_{nap}$)] complex underwent oxygen insertion with TBHP in ^{t}BuOH solution (Eq. (2)) whereas [Pd(L$^1{}_{nap}$)] required $VO(acac)_2$ along with TBHP for effective oxygen insertion (Eq. (3)).

Milder and greener reagent containing Mixture of aqueous hydrogen peroxide and dichloromethane afforded oxygenated product only in the case of [Ni(L$^1{}_{nap}$)] at room temperature (Eq. (2)). Therefore, in general, C–O bond formation after ortho C–H bond activation is more facile for nickel acetate than the sodium tereachloro palladate. Isolation and unequivocal characterization of [Ni(L$^1{}_{nap}$)] than [Pd(L$^1{}_{nap}$)] complexes provided the necessary evidence in favor of ortho C–H cleavage prior to C–O bond formation to predict the plausible mechanism.

*2.3. Preparation of authentic $H_2OL^1{}_{nap}$, **9**, and their complexes*

Authentic $H_2OL^1{}_{nap}$ ligand was synthesized by the condensation of HOL^1–NH_2 with 2-hydroxy-1-napthaldehyde as shown in Eq. (4). HOL^1–NH_2 was prepared by the procedure described earlier [4,6]. Subsequently authentic $H_2OL^1{}_{nap}$ was utilized for the preparation of [Ni(OL$^1{}_{nap}$)] and [Pd(OL$^1{}_{nap}$)] complexes upon reaction with $Ni(OAc)_2{\cdot}4H_2O$ and Na_2PdCl_4 respectively in methanol. Characterization data, spectral features and other physical characteristics of these complexes were identical with the products obtained after oxidation of [Ni(L$^1{}_{nap}$)] and [Pd(L$^1{}_{nap}$)] with peroxo reagents (see above).

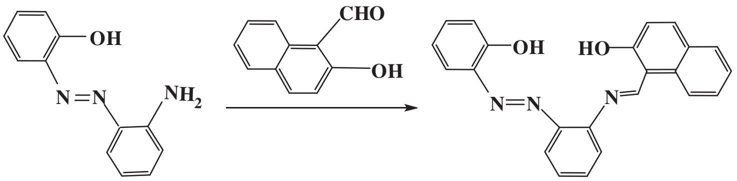

9
$H_2OL^1{}_{nap}$ (4)

2.4. Characterization

All the H_2L_{nap}, **4**, ligands displayed characteristic UV–Vis spectra in dichloromethane solution with absorptions near 465 nm and near 315 nm [4–8]. In dichloromethane solution [Ni(L$^1{}_{nap}$)] complexes, **5**, exhibited low energy absorption near 620 nm and [Pd(L_{nap})] complexes, **6**, displayed characteristic UV–Vis spectra having several structured absorption bands within 250–450 nm. The orange solution of authentic $H_2OL^1{}_{nap}$ in dichloromethane displayed overlapped absorptions within 420–320 nm. Oxidised com-

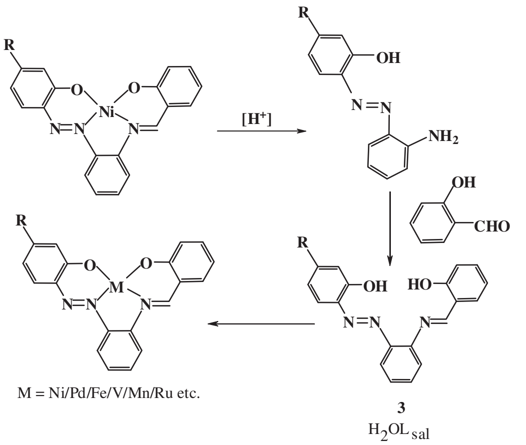

Scheme 2.

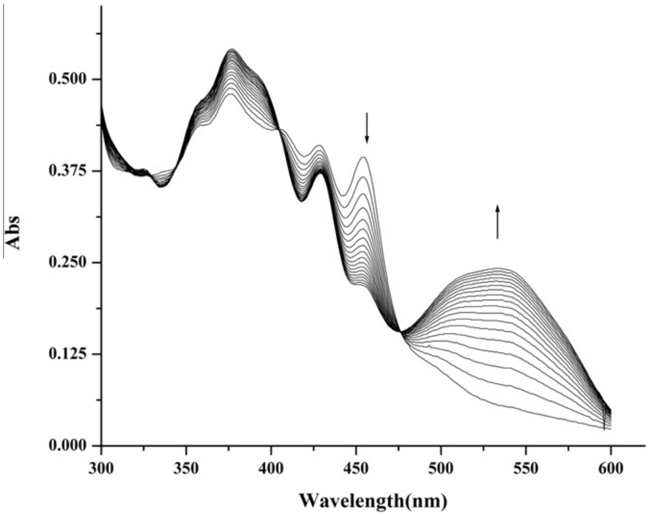

Fig. 1. Graphical change in UV–Vis spectra during oxidation of [Pd(L^1_{nap})] to [Pd(OL^1_{nap})] by *m*CPBA. Concentration of complex was 2.63×10^{-5}(M) and of *m*CPBA was 4.6×10^{-4}(M).

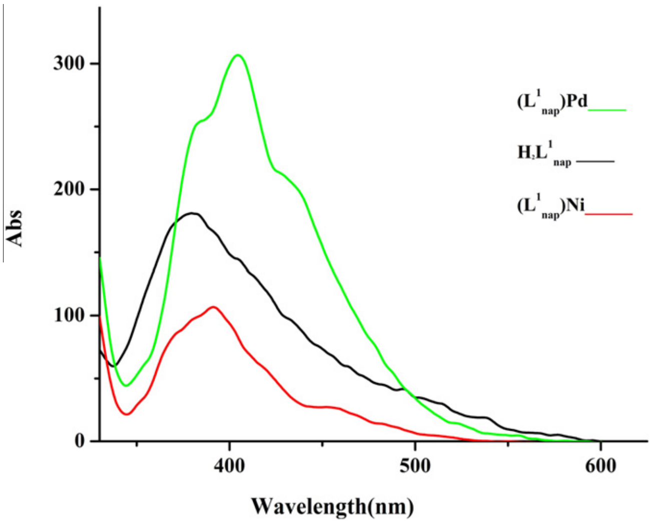

Fig. 2. Emission spectra of $H_2L^1_{nap}$, [Pd(L^1_{nap})] and [Ni(L^1_{nap})].

plexes, [Ni(OL^1_{nap})] exhibited low energy bands at 630 and 520 nm whereas [Pd(OL^1_{nap})] showed one absorption with maxima at 530 nm. Relevant data are included in Section 4.

In the IR spectra, the $\nu_{N=N}$ band of H_2L_{nap} ligands (near 1482 cm^{-1}) shifted to lower frequency (1353–1361 cm^{-1}) after formation of [Ni(L_{nap})] and [Pd(L_{nap})] chelates, consistent with the coordination of the azo nitrogen [4–8,20]. The $\nu_{C=N}$ band within 1615–1624 cm^{-1} of the H_2L_{nap} ligands moved to 1613–1616 cm^{-1} region in [Ni(L_{nap})] and [Pd(L_{nap})] complexes. A broad signal near 3290 cm^{-1} for ν_{OH} of H_2L_{nap} was absent in the spectra of the complexes signifying the dissociation of –OH proton and its coordination to the metal centre as O^- [4–8,20]. The $\nu_{N=N}$ (1473 cm^{-1}) of $H_2OL^1_{nap}$ shifted to lower frequency in [Ni (OL^1_{nap})] and [Pd(OL^1_{nap})] at 1372 and 1375 cm^{-1}, respectively. The $\nu_{C=N}$ bands of $H_2OL^1_{nap}$ (1628 cm^{-1}) appeared within 1603–1605 cm^{-1} in complexes. Relevant data are collected in Section 4.

A repeat ^1H NMR experiments of the H_2L_{nap} ligands exhibited two doublets near δ 15.9 (for $H_2L^1_{nap}$ and $H_2L^3_{nap}$) and δ 9.16, whereas $H_2L^2_{nap}$ displayed a broad signal at δ 15.87 and a doublet at δ 9.16. Therefore a revisit to the ^1H NMR spectra of H_2L_{nap} became necessary [7]. Rationale of these resonances has been realized by considering the intramolecular hydrogen bonded structures shown in **I**. The doublet near δ 15.9 for $H_2L^1_{nap}$ and $H_2L^3_{nap}$ were assigned for hydrogen bonded –OH.

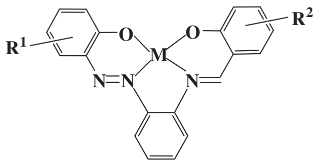

1

Doublet nature was attributed to coupling with aldimino –C–H proton through imino nitrogen as shown in **I**. On the other hand the aldimine –C–H proton appears near δ 9.20 as a doublet indicating significant coupling with the hydrogen bonded proton on N. This rationale can be supported by the fact that the doublet resonance for aldimino proton appeared as sharp singlet near δ 9.16 on D_2O shaking. Crystal structure of $H_2L^1_{nap}$ indicated the intramolecular hydrogen bond in solid state also (see below).

The ^1H NMR spectra of [Ni(L_{nap})] and [Pd(L_{nap})] complexes did not display any –OH resonance near δ 15.9 signifying the dissociation of –OH proton and its coordination to the metal centre as phenoxide and the aldimino (–N=CH–) proton resonance appear as a sharp singlet near δ 9.40. The proton counts obtained from ^1H NMR spectra and the spectral patterns of the cyclometallated complexes are consistent with their formula and structures in

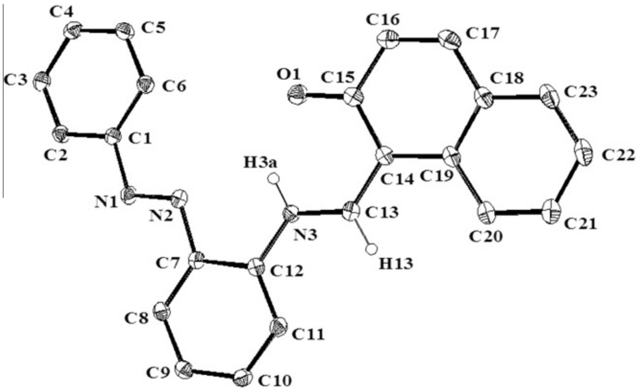

Fig. 3. Perspective view of $H_2L^1_{nap}$ with atom numbering scheme. Hydrogen atoms (except H3a and H13) are omitted for clarity.

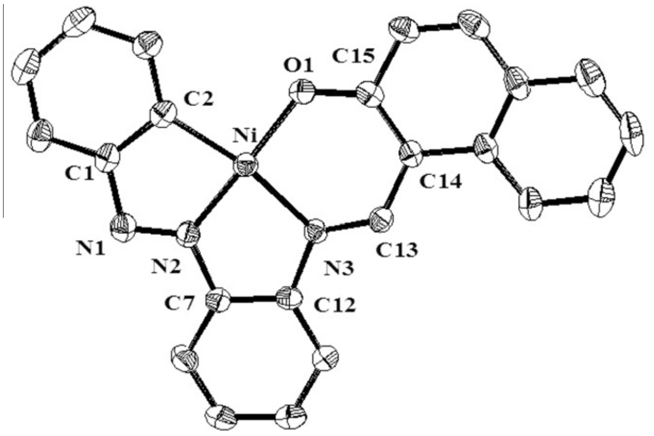

Fig. 4. Perspective view of [Ni(L^1_{nap})] with atom numbering scheme. Hydrogen atoms are omitted for clarity.

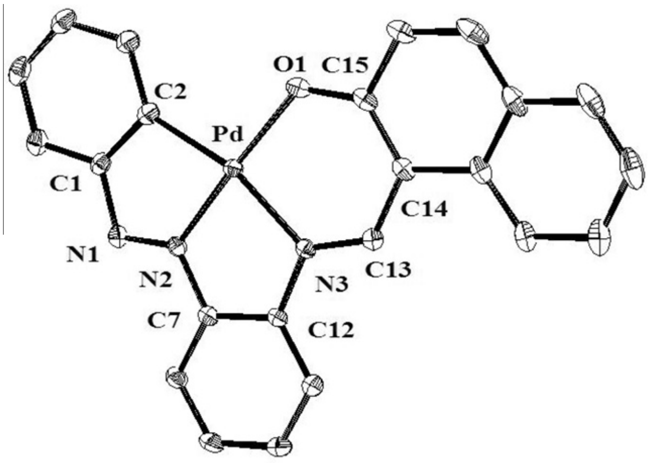

Fig. 5. Perspective view of [Pd(L^1_{nap})] with atom numbering scheme. Hydrogen atoms are omitted for clarity.

Table 1
Selected bond distances (Å) and angles (°) for $H_2L^1_{nap}$, **4a**.

Bond distances			
O1–C15	1.2630(18)	C14–C15	1.4533(19)
N1–N2	1.2556(16)	C14–C19	1.4627(18)
N1–C1	1.4269(18)	N3–C13	1.3298(17)
N2–C7	1.4233(18)	N3–H3a	0.8595
N3–C12	1.4040(16)	C1–C2	1.3926(18)
Bond angles			
N2–N1–C1	114.64(11)	N3–C12–C7	118.04(12)
N1–N2–C7	113.66(11)	N3–C12–C11	122.57(12)
C12–N3–C13	126.25(12)	N3–C13–C14	124.10(13)
C13–N3–H3a	116.87	N2–C7–C12	115.40(11)
C12–N3–H3a	116.88	N2–C7–C8	124.77(12)
N1–C1–C6	125.20(12)	O1–C15–C14	122.48(13)
C2–C1–C6	120.46(13)	C1–C2–C3	120.16(12)
N1–C1–C2	114.34(11)	O1–C15–C16	120.08(13)

Table 2
Selected bond distances (Å) and angles (°) for [Ni(L^1_{nap})], **5a**.

Bond distances			
Ni–O1	1.8204(17)	C11–C12	1.385(4)
Ni–N2	1.799(2)	C15–C16	1.426(4)
Ni–N3	1.884(2)	N1–N2	1.284(3)
Ni–C2	1.880(2)	N1–C1	1.404(3)
O1–C15	1.303(3)	N3–C13	1.300(3)
N2–C7	1.419(3)	N3–C12	1.422(3)
Bond angles			
O1–Ni–N2	177.98(10)	Ni–N2–N1	123.91(17)
O1–Ni–N3	96.05(8)	Ni–N2–C7	116.21(17)
O1–Ni–C2	96.18(10)	N1–N2–C7	119.9(2)
N2–Ni–N3	85.58(9)	Ni–N3–C12	112.24(15)
N2–Ni–C2	82.16(11)	Ni–N3–C13	125.85(17)
N3–Ni–C2	167.69(10)	N1–C1–C6	120.3(2)
Ni–O1–C15	126.07(16)	Ni–C2–C1	110.07(18)
N2–N1–C1	107.5(2)	N1–C1–C2	116.4(2)
O1–C15–C16	115.8(2)	Ni–C2–C3	133.4(2)

Table 3
Selected bond distances (Å) and angles (°) for [Pd(L^1_{nap})], **6a**.

Bond distances			
Pd–O1	1.9939(15)	C7–C12	1.422(3)
Pd–N2	1.9172(17)	C8–C9	1.383(3)
Pd–N3	2.0131(15)	C9–C10	1.390(3)
Pd–C2	1.992(2)	C10–C11	1.376(3)
O1–C15	1.312(3)	C11–C12	1.399(3)
N1–N2	1.278(2)	C13–C14	1.421(3)
N1–C1	1.408(3)	N3–C12	1.420(3)
N2–C7	1.420(3)	N3–C13	1.314(2)
Bond angles			
O1–Pd–N2	176.56(7)	Pd–C2–C1	109.25(15)
O1–Pd–N3	93.76(6)	Pd–C2–C3	134.33(16)
O1–Pd–C2	102.73(7)	N1–N2–C7	121.45(17)
N2–Pd–N3	83.71(6)	Pd–N3–C12	111.05(11)
N2–Pd–C2	79.71(8)	Pd–N3–C13	125.18(14)
N3–Pd–C2	163.31(7)	N2–C7–C8	124.19(19)
Pd–O1–C15	123.23(13)	Pd–N2–N1	123.40(13)
N2–N1–C1	108.89(16)	Pd–N2–C7	115.14(12)

solution. The ^1H NMR data for all the ligands and complexes are given in Section 4.

The ^1H NMR results of authentic $H_2OL^1_{nap}$ ligand exhibited two singlets at δ 12.39, δ 10.76 for two phenolic protons and at δ 9.33 for one aldimino C–H proton. Resonances for other fourteen aromatic protons appeared within δ 7.0–8.1. Corresponding [Pd(OL^1_{nap})] and [Ni(OL^1_{nap})] complexes, prepared by reacting $H_2OL^1_{nap}$ with Na_2PdCl_4 and $Ni(OAc)_2$ respectively, did not display the resonances for two phenolic protons consistent with phenolato binding. The aldimino C–H appeared as singlets at δ 9.60 for [Pd(OL^1_{nap})] and at δ 9.29 for [Ni(OL^1_{nap})]. All other resonances for aromatic protons appeared as overlapped signals within δ 6.8–8.4. The ^1H NMR of oxidized products of [Ni(L^1_{nap})] and [Pd(L^1_{nap})] matched well with the authentic complexes.

2.5. Emission spectra

The π-conjugated chromophore containing ligand, $H_2L^1_{nap}$, **4a**, exhibited emission maxima at 380 nm in dilute dichloromethane solution (10^{-5} M) when excited at 320 nm. In dichloromethane solution (10^{-5} M), The Ni(II) complex, [(L^1_{nap})Ni], exhibited quenched emission at 390 nm but the emission intensity of Pd(II) complex, [Pd(L^1_{nap})], was larger than the corresponding ligand at 405 nm. The emission spectra of $H_2L^1_{nap}$, [Ni(L^1_{nap})] and [Pd(L^1_{nap})] are shown in Fig. 2. The augmented emission intensity of Pd(II) complex can be attributed to chelation-enhanced fluorescence (CHEF) [10,11]. Whereas decrease in emission intensity for Ni(II) complex can be ascribed as “heavy atom effect” [9,21]. It was mentioned elsewhere that the “heavy atom effect” does not induce CHEF and causes the quenching through two well defined mechanism – either naphthyl→metal energy transfer (ET) or metal→naphthyl electron transfer (et) [10,11].

2.6. X-ray structures

Unequivocal characterizations of the ligands, H_2L_{nap}, and corresponding metal complexes, $(L_{nap})M$ (M = Ni, Pd), were performed by X-ray structure analysis of $H_2L^1{}_{nap}$, $[Ni(L^1{}_{nap})]$ and $[Pd(L^1{}_{nap})]$ respectively. Figs. 3–5 show perspective views of their molecular structures. Tables 1–3 respectively contain the selected bond distances and angles. The X-ray structure of $H_2L^1{}_{nap}$ reveals the planar geometry of the ligand. All the non hydrogen atoms of $H_2L^1{}_{nap}$ make a good plane (mean deviation 0.251 Å). The N(1)–C(1), (1.4266(18) Å); N(2)–C(7), (1.4237(18) Å) and N(3)–C(12), (1.4039(17) Å) lengths of the free ligand are close to C–N single bond length. The N(3)–C(13) length (1.3309(17) Å) is similar to the imine (C=N) distance [4–8,22–25]. The N(1)–N(2) length (1.2556(16) Å) is very similar to azo (–N=N–) bond length [4–8,22–25]. The distance (2.577 Å) between aryl O(1) and aldimine N(3) signify the intramolecular H-bond [19–26]. H(3a) was located by Fourier mapping indicating significant interaction with imine nitrogen giving rise to considerable coupling with aldimine (–N=CH–) proton as observed in ^{1}H NMR spectra of the ligands (*vide supra*). In the X-ray structures of metal complexes the dinegative anion of ligands, $(L_{nap})^{2-}$ bind Ni(II) and Pd(II) in distorted square planer geometry. The $[Ni(L^1{}_{nap})]$molecule has a planar structure with a maximum deviation of 0.131 Å from the least square plane. The planar molecules $[Ni(L^1{}_{nap})]$ in the asymmetric units are held as weak staggered unsupported dimers where Ni–Ni distances are 3.410 Å. The dimers are arranged in a stair-like manner where the inter dimer Ni–Ni distance is 6.837 Å. The Ni–N(azo) [Ni–N2; 1.799(2) Å] and Ni–N(imine) [Ni–N3; 1.884(2) Å] distances are different due to stronger trans influence of aryl carbon than the phenolic oxygen [4]. The Ni–C2 distance (1.880(2) Å) is comparable with Ni–C distance of orthometallated Ni(II) complex of azobenzene [17]. Ni–O1 distance (1.8204(17) Å) is within the normal range of Ni–O distances (1.83(1) Å) in *salen* complexes [27,28]. The X-ray structure of palladium complex, $[Pd(L^1{}_{nap})]$, was similar to $[Ni(L^1{}_{nap})]$. Pd–C (1.993(2) Å) and Pd–O (1.9949(15) Å) distances are within the normal range [6,29,30]. Between the Pd–N(azo) (1.9175(17) Å) and Pd–N(im) (2.0156(16) Å) distances, the former is shorter due to either stronger π-backbonding or stronger trans influence of carbon than the phenoxide oxygen [6]. In general, all the metal–ligand bond distances of $[Pd(L^1{}_{nap})]$ are larger than those in $[Ni(L^1{}_{nap})]$ complex due to larger size of Pd(II) than Ni(II).

3. Conclusion

Orthometallated complexes, of Ni(II) and Pd(II) have been prepared with a naphthyl moiety within the ligand framework. All the orthometallated complexes underwent oxygen insertion upon rection with peroxy acids to form the complexes incorporating azo ligands having *salen* like coordination sites –(O, N, N, O). Luminescence properties of the complexes and ligands are discussed considering heavy atom effect and "chelation enhanced fluoroscence (CHEF)". The oxygenated products display very weak emission.

4. Experimental

4.1. Materials

The solvents used in the reactions were of reagent grade obtained from Merck, Kolkata, India and purified and dried by reported procedures [31]. 2-(Arylazo)anilines and 1-{[2-(arylazo)phenyl]iminomethyl}-2-naphthol were prepared according to reported procedure [7,22,31]. Palladium chloride, nickel acetate tetra hydrate were purchased from Merck, Kolkata, India. Sodiumtetrachloropalladate (II) was prepared by reported procedure [22].

4.2. Physical measurements

Microanalyses (C, H, N, O/S) were performed using a Perkin-Elmer 2400 elemental analyzer. Infrared spectra were recorded on a Perkin-Elmer L120-00A FT-IR spectrometer with the samples prepared as KBr pellets. Electronic spectra were recorded on a Shimadzu UV-1800 & UV-2401PC spectrophotometer. ^{1}H NMR spectra were obtained on Bruker RPX 500 NMR & Bruker DPX 400 spectrometers in $CDCl_3$.

4.3. Syntheses of compounds

4.3.1. Synthesis of $[Ni(L^1{}_{nap})]$ complex (***5a***)

A solution of $H_2L^1{}_{nap}$ (0.2 g, 0.57 mmol) in 10 cm^3 methanol was added to a 5 cm^3 methanolic solution of $Ni(OAc)_2{\cdot}4H_2O$ (0.142 g, 0.57 mmol). The mixture was then heated to reflux for 12 h to obtain green precipitate of $[Ni(L^1{}_{nap})]$complex. The solid product was then filtered and washed with methanol. The volume of the filtrate was reduced to ~10 cm^3 and kept in a beaker covering with a glass. It was kept for few days. A little more crop of product was collected.

5a*:* Yield: 0.258 g (65%). *Anal.* Calc. for $C_{23}H_{15}N_3NiO$ (408.07): C, 67.6; H, 3.7; N, 10.2. Found: C, 67.7; H, 3.6; N, 10.3%. UV–Vis (CH_2Cl_2): [λ_{max}, nm (ε, M^{-1} cm^{-1})]: 622 (434), 478 (4644), 356 (5945). IR (KBr): 1374 (N=N); 1605 (C=N). ^{1}H NMR ($CDCl_3$): δ = 9.49 (s, 1H; N=CH), 8.02 (d, 1H; Ar), 7.66–7.62 (m, 5H; Ar), 7.48 (t, 1H; Ar), 7.43–7.27 (m, 4H; Ar), 7.12–7.08 (m, 3H; Ar) ppm.

4.3.2. Synthesis of $[Ni(L^2{}_{nap})]$ (***5b***) and $[Ni(L^3{}_{nap})]$ (***5c***)

Complexes $[Ni(L^2{}_{nap})]$ and $[Ni(L^3{}_{nap})]$ were prepared using the ligand $H_2L^2{}_{nap}$ and $H_2L^3{}_{nap}$ in place of $H_2L^1{}_{nap}$, respectively.

5b*:* Yield: 0.276 g (70%). *Anal.* Calc. for $C_{24}H_{17}N_3NiO$ (422.07): C, 68.2; H, 4.0; N, 9.9. Found: C, 68.3; H, 4.0; N, 9.9%. UV–Vis (CH_2Cl_2): [λ_{max}, nm (ε, M^{-1} cm^{-1})]: 623 (1207), 480 (12 691), 380 (15 012). IR (KBr): 1378 (N=N), 1603 (C=N). ^{1}H NMR ($CDCl_3$): δ = 9.44 (s, 1H; N=CH), 7.98 (d, 1H; Ar), 7.63–7.47 (m, 6H; Ar), 7.36 (t, 1H; Ar), 7.14–7.06 (m, 4H; Ar), 6.87 (d, 1H; Ar), 2.43 (s, 3H; Me) ppm.

5c*:* Yield: 0.255 g (60%). *Anal.* Calc. for $C_{23}H_{14}N_3NiOCl$ (443.57): C, 62.4; H, 3.1; N, 9.4. Found: C, 62.4; H, 3.2; N, 9.4%. UV–Vis (CH_2Cl_2): [λ_{max}, nm (ε, M^{-1} cm^{-1})]: 622 (729), 475 (7851), 384 (10 212). IR (KBr pellets, cm^{-1}): 1375 (N=N), 1602 (C=N). ^{1}H NMR ($CDCl_3$): δ = 9.40 (s, 1H; N=CH), 7.96 (d, 1H; Ar), 7.63 (d, 2H; Ar), 7.57 (t, 2H; Ar), 7.50–7.46 (m, 3H; Ar), 7.41 (t, 1H; Ar), 7.09 (t, 2H; Ar), 7.05 (d, 1H; Ar) ppm.

4.3.3. Synthesis of $[Pd(L^1{}_{nap})]$ complex (***6a***)

A solution of $H_2L^1{}_{nap}$ (0.2 g, 0.57 mmol) in 10 cm^3 methanol was added to a 5 cm^3 methanolic solution of Na_2PdCl_4 (0.168 g, 0.57 mmol). The mixture was then stirred for 20 h to obtain brown precipitate of $[Pd(L^1{}_{nap})]$ complex. The solid product was then filtered and washed with methanol. The product was then purified by preparative TLC using benzene–acetonitrile (19:1) mixed solvent. Upon evaporation of solvent, the pure desired brown complex $[Pd(L^1{}_{nap})]$ was isolated.

6a*:* Yield: 0.310 g (65%). *Anal.* Calc. for $C_{23}H_{15}N_3PdO$ (455.80): C, 60.6; H, 3.3; N, 9.2. Found: C, 60.5; H, 3.3; N, 9.2%. UV–Vis (CH_2Cl_2): [λ_{max}, nm (ε, M^{-1} cm^{-1})]: 450 (5068), 374 (5908), 274 (9835), 245 (11 611). IR (KBr pellets, cm^{-1}): 1357 (N=N), 1603 (C=N). ^{1}H NMR ($CDCl_3$): δ = 9.54(s, 1H; N=CH), 8.03 (d, 1H; Ar), 7.79 (d, 1H; Ar), 7.75 (d, 2H; Ar), 7.68 (d, 1H; Ar) 7.64 (d, 1H; Ar), 7.54–7.41 (m, 4H; Ar), 7.35 (d, 2H; Ar), 7.26–7.13 (m, 2H; Ar) ppm.

*4.3.4. Synthesis of[Pd ($L^2{}_{nap}$)] (**6b**) and [Pd($L^3{}_{nap}$)] (**6c**)*

Complexes [Pd($L^2{}_{nap}$)] and [Pd($L^3{}_{nap}$)] were prepared using the ligands $H_2L^2{}_{nap}$ and $H_2L^3{}_{nap}$ in place of $H_2L^1{}_{nap}$, respectively.

***6b**:* Yield: 0.260 g (55%). *Anal.* Calc. for $C_{24}H_{17}N_3PdO$ (469.80): C, 61.3; H, 3.6; N, 8.9. Found: C, 61.3; H, 3.6; N, 8.9%. UV–Vis (CH_2Cl_2): [λ_{max}, nm (ε, M^{-1} cm^{-1})]: 450 (4788), 374 (5321), 274 (8376), 245 (9819). IR (KBr pellets, cm^{-1}): 1353 (N=N); 1602 (C=N). ^1H NMR ($CDCl_3$): δ = 9.40 (s, 1H; N=CH), 8.19 (d, 1H; Ar), 8.08–8.04 (m, 1H; Ar), 7.92 (d, 1H; Ar) 7.67–7.56 (m, 3H; Ar), 7.40–7.26 (m, 2H; Ar), 7.22–7.12 (m, 2H; Ar), 7.05 (t, 2H; Ar), 6.84 (d, 1H; Ar), 2.28(s, 3H; Me) ppm.

***6c**:* Yield: 0.234 g (50%). *Anal.* Calc. for $C_{23}H_{14}N_3PdOCl$ (491.30): C, 56.3; H, 2.8; N, 8.5. Found: C, 56.3; H, 2.8; N, 8.6%. UV–Vis (CH_2Cl_2): [λ_{max}, nm (ε, M^{-1} cm^{-1})]: 450 (5044), 374 (5960), 274 (8940), 245 (10440). IR (KBr): 1353 (N=N), 1602 (C=N). ^1H NMR ($CDCl_3$): δ = 9.38(s, 1H; N=CH), 7.94 (d, 1H; Ar), 7.68 (d, 1H; Ar), 7.62 (d, 2H; Ar), 7.58 (d, 1H; Ar), 7.54 (d, 2H; Ar), 7.47–7.40 (m, 3H; Ar), 7.13 (t, 1H; Ar), 7.06–7.03 (m, 2H; Ar) ppm.

*4.4. Synthesis of complex, ($OL^1{}_{nap}$)Ni (**7**)*

The details for the preparation of ($OL^1{}_{nap}$)Ni are given.

4.4.1. Reaction of [Ni($L^1{}_{nap}$)] with mCPBA

A solution of *m*CPBA (0.143 g, 0.824 mmol) in dichloromethane (5 mL) was added drop wise to a stirred solution of [Ni($L^1{}_{nap}$)] (0.100 g, 0.245 mmol) in dichloromethane (25 mL). Immediately the color of the solution began to change from deep green to brown. The stirring was continued for 10 min. Evaporation of the solvent in vacuo afforded a brown solid mass. The solid mass was washed with diethyl ether (3‴5 mL). The product was then purified by preparative TLC using a benzene/acetonitrile (19:1) mixture as eluent. Upon evaporation of the solvent, the pure target complex [Ni($OL^1{}_{nap}$)] was obtained.

4.4.2. Reaction of ($L^1{}_{nap}$)Ni with TBHP

To a stirred solution of [Ni($L^1{}_{nap}$)] (0.571 g, 0.140 mmol) in 25 cm^3 dichloromethane or *tert*-butanol, TBHP (0.30 mL, 2.76 mmol) was added dropwise. Immediately the color of the solution began to turn from deep green to brown. The stirring was continued for 30 min. Evaporation of the solvent under vaccuo afforded a brown solid mass. The solid mass, thus obtained, was washed with water and diethyl ether. The product was then purified by preparative TLC using benzene–acetonitrile (19:1) mixed solvent. Upon evaporation of solvent the pure desired complex [Ni($OL^1{}_{nap}$)] was obtained.

4.4.3. Reaction of [Ni($L^1{}_{nap}$)] with H_2O_2

To a stirred solution of [Ni($L^1{}_{nap}$)] (0.34 g, 0.083 mmol) in 15 cm^3 dichloromethane, 10 cm^3 of 6% H_2O_2 was added drop wise. The color of the organic layer began to turn from deep green to brown after 15 min. The stirring was continued for 45 min. Evaporation of the organic solvent, after separation from the aqueous layer, under vaccuo afforded a dark solid mass. The solid mass, thus obtained, was washed with water. The product was then purified by preparative TLC using benzene–acetonitrile (19:1) mixed solvent. Upon evaporation of solvent the pure desired complex [Ni($OL^1{}_{nap}$)] was obtained.

Yield: 0.205 g (70%). *Anal.* Calc. for $C_{23}H_{15}N_3NiO_2$ (424.07): C, 65.1; H, 3.5; N, 9.9. Found: C, 65.1; H, 4.0; N, 9.9%. UV–Vis (CH_2Cl_2): [λ_{max}, nm (ε, M^{-1} cm^{-1})]: 646 (8935), 531 (2207), 478 (4516), 353 (6014), 256 (11523). IR (KBr): 1371 (N=N); 1603 (C=N). ^1H NMR ($CDCl_3$): δ = 9.29 (s, 1H; N=CH), 8.22 (d, 1H; Ar), 8.08 (d, 1H; Ar), 7.84 (d, 1H; Ar), 7.78 (d, 1H; Ar), 7.70 (t, 2H; Ar), 7.54 (t, 1H; Ar), 7.43–7.39 (m, 2H; Ar), 7.36–7.35 (m, 2H; Ar), 7.30–7.22 (m, 1H; Ar), 6.89 (t, 1H; Ar) ppm.

Table 4
Crystallographic data for $H_2L^1{}_{nap}$, **4a**, [Ni($L^1{}_{nap}$)], **5a** and [Pd($L^1{}_{nap}$)], **6a**.

Chemical formula	$C_{23}H_{17}N_3O$	$C_{23}H_{15}N_3NiO$	$C_{23}H_{15}N_3PdO$
Formula weight	351.40	408.07	455.80
Space group	$P2_12_12_1$ (No. 19)	$P21/n$ (No. 14)	$P21/n$ (No. 14)
Crystal system	orthorhombic	monoclinic	monoclinic
a (Å)	5.5597(2)	12.4865(2)	12.5071(7)
b (Å)	11.3742(5)	8.6827(2)	8.5743(5)
c (Å)	27.1976(13)	17.2322(3)	17.4363(10)
α (°)	90	90	90
β (°)	90	109.8440(10)	109.8980(10)
γ (°)	90	90	90
λ (Å)	0.71073	0.71073	0.71073
V ($Å^3$)	1719.90(13)	1757.32(6)	1758.23(17)
Z	4	4	4
T (K)	293	293	293
D_{calc} (Mg/m^3)	1.357	1.542	1.722
μ (mm^{-1})	0.085	1.123	1.075
$F(000)$	736	840	912
R[all data]	0.0354	0.0302	0.0240
$wR_2[I > 2\sigma(I)]$	0.0973	0.0712	0.0615
Goodness-of-fit GOF on F^2	1.08	1.03	1.05

*4.5. Syntheses of complex, [Pd($OL^1{}_{nap}$)] (**8**)*

The details for the preparation of [Pd($OL^1{}_{nap}$)] are given.

4.5.1. Reaction of [Pd ($L^1{}_{nap}$)] with mCPBA

A solution of (0.144 g, 0.824 mmol) mCPBA was added dropwise to a stirred solution of [Pd($L^1{}_{nap}$)] (0.100 g, 0.219 mmol) in 25 mL dichloromethane. Immediately, the color of the solution began to change from brown to pink. The stirring was continued for 30 min. Evaporation of the solvent under vaccuo afforded a pink solid mass. The solid mass thus obtained was washed thrice with diethyl ether, taking 5 mL for each wash. The product was then purified by preparative TLC using benzene as the eluent. The pink band was collected.

4.5.2. Reaction of [Pd ($L^1{}_{nap}$)] with TBHP

To a stirred solution of [Pd($L^1{}_{nap}$)] (0.100 g, 0.219 mmol) in 25 cm^3 dichloromethane or *tert*-butanol, TBHP (0.40 mL, 3.68 mmol) was added drop wise in presence of catalytic amount VO(acac)$_2$. Immediately the color of the solution began to turn from brown to pink. The stirring was continued for 1 h. Evaporation of the solvent under vaccuo afforded a pink solid mass. The solid mass, thus obtained, was washed with water and diethyl ether. The product was then purified by preparative TLC using benzene–acetonitrile (19:1) mixed solvent. Upon evaporation of solvent the pure desired complex [Pd ($OL^1{}_{nap}$)] was obtained.

Yield**:** 0.138 g (50%). *Anal.* Calc. for $C_{23}H_{15}N_3PdO_2$ (471.80): C, 58.5; H, 3.2; N, 8.9. Found: C, 58.5; H, 3.2; N, 8.8%. UV–Vis (CH_2Cl_2): [λ_{max}, nm (ε, M^{-1} cm^{-1})]: 538 (3779), 420 (3400), 379 (6100), 244 (12100). IR (KBr): 1384 (N=N), 1605 (C=N). ^1H NMR ($CDCl_3$): δ = 9.58 (s, 1H; N=CH), 8.36 (d, 1H; Ar), 8.11 (d, 1H; Ar), 7.98 (d, 1H; Ar), 7.90 (d, 1H; Ar) 7.76 (d, 1H; Ar), 7.56–7.50 (m, 1H; Ar), 7.48–7.39 (m, 2H; Ar), 7.36–7.7.34 (m, 2H; Ar), 7.33–7.30 (m, 2H; Ar), 6.87 (m, 1H; Ar).

*4.6. Syntheses of authentic $H_2OL^1{}_{nap}$, **9***

To a solution of (0.100 g, 0.469 mmol) HOL^1–NH_2 in 50 cm^3 diethyl ether 2-hydroxy 1-napthaldehyde (0.0573 g, 0.333 mmol) was added. The mixture of solution was heated to reflux for 12 h.

The solvent was evaporated in vaccuo. The solid product was kept in a vacuum desiccator for 24 h before use and characterization.

Yield: 0.155 g (90%). *Anal.* Calc. for $C_{23}H_{17}N_3O_2$ (367): C, 75.2; H, 4.6; N, 11.4. Found: C, 75.1; H, 4.6; N, 11.5%. UV–Vis (CH_2Cl_2): [λ_{max}, nm (ε, M^{-1} cm^{-1})]: 320 (30000), 232 (53000). IR (KBr): 1473 (N=N), 1628 (C=N). ^1H NMR ($CDCl_3$): δ = 12.39 (s, OH), 10.76 (s, OH), 9.33 (s, 1H; N=CH), 8.046 (d, 1H; Ar), 7.97 (d, 1H; Ar), 7.90 (d, 1H; Ar), 7.76 (d, 1H; Ar) 7.65 (d, 1H; Ar), 7.49 (t, 2H; Ar), 7.44 (t, 1H; Ar), 7.34 (d, 2H; Ar), 7.28–7.22 (m, 3H; Ar), 7.10 (d, 1H; Ar), 7.02–6.98 (m, 2H; Ar).

4.7. Syntheses of authentic [Ni(OL^1_{nap})], **7**

A stirred solution of $Ni(OAc)_2{\cdot}4H_2O$ (0.067 g, 0.272 mmol) in methanol (5 mL), solution of $H_2OL^1_{nap}$ (0.100 g, 0.272 mmol) in methanol (10 mL). The color of the solution changes from deep green to brown. The stirring was continued for 10 min. Evaporation of the solvent in vacuo afforded a brown solid mass. The product was then purified by preparative TLC using a benzene/acetonitrile (19:1) mixture as eluent. Upon evaporation of the solvent, the pure target complex [Ni(OL^1_{nap})] was obtained.

4.8. Syntheses of authentic [Pd(OL^1_{nap})], 8

(0.100 g, 0.272 mmol) solution of $H_2OL^1_{nap}$ in methanol (10 mL) added dropwise to a stirred solution of (0.100 g, 0.219 mmol) Na_2PdCl_4 in 5 mL methanol. The color of the solution began to change from brown to pink. The stirring was continued for 30 min. Evaporation of the solvent under vaccuo afforded a pink solid mass. The product was then purified by preparative TLC using benzene as the eluent. The pink band was collected. Upon evaporation of the solvent, the pure target complex [Pd(OL^1_{nap})] was obtained.

5. Crystallography

Data for the crystals $H_2L^1_{nap}$, **4a**, [Ni(L^1_{nap})], **5a** and [Pd(L^1_{nap})], **6a** were collected by the ω-scan technique on a Brucker smart CCD diffractometer with Mo Kα radiation monochromated by a graphite crystal. The structure was solved by direct method with SHELXS-97 program. Full matrix least square refinements were performed using the SHELX-97 program (PC version) [32,33]. All non-hydrogen atoms were refined anisotropically using reflections $I > 2\sigma(I)$. Hydrogen atoms were included at the calculated positions. The crystal data and data collection parameters for $H_2L^1_{nap}$, [Ni(L^1_{nap})] and [Pd(L^1_{nap})] are listed in Table 4.

Acknowledgments

We are thankful to the DST (New Delhi) for funding and fellowship to PP under DST-WOS-A project (No. SR/WOS-A/CS-140/2011). The necessary laboratory and infrastructural facility are provided by the Dept. of Chemistry, University of Kalyani. The support of DST under FIST program to the Department of Chemistry, and PURSE to the University of Kalyani is acknowledged.

Appendix A. Supplementary material

CCDC 889016, 889017 and 889018 contain the supplementary crystallographic data for$H_2L^1_{nap}$, [Ni(L^1_{nap})] and [Pd(L^1_{nap})], respectively. These data can be obtained free of charge via http://www.ccdc.cam.ac.uk/conts/retrieving.html, or from the Cambridge Crystallographic Data Centre, 12 Union Road, Cambridge CB2 1EZ, UK; fax: +44 1223 336 033; or e-mail: deposit@ccdc.cam.ac.uk. Figs. S1–S18 show the UV–Vis and IR spectra Figs. S19–S31 show ^1H NMR spectra of all the ligands and complexes. Supplementary data associated with this article can be found, in the online version, at http://dx.doi.org/10.1016/j.poly.2012.12.011.

References

[1] (a) T.W. Lyons, M.S. Sanford, Chem. Rev. 110 (2010) 1147;
(b) D.A. Colby, R.G. Bergman, J.A. Ellman, Chem. Rev. 110 (2010) 624;
(c) P. Sehnal, R.J.K. Taylor, I.J.S. Fairlamb, Chem. Rev. 110 (2010) 824.
[2] (a) F. Kakiuchi, T. Kochi, Synthesis (2008) 3013;
(b) L.-M. Xu, B.-J. Li, Z. Yang, Z.-J. Shi, Chem. Soc. Rev. 39 (2010) 712;
(c) L. Ackermann, Chem. Commun. 46 (2010) 4866.
[3] (a) H. Shiota, Y. Ano, Y. Aihara, Y. Fukumoto, N. Chatani, J. Am. Chem. Soc. 133 (2011) 14952;
(b) I. Omae, Chem. Rev. 79 (1979) 287;
(c) A. Nishimura, M.Ohashi, S. Ogoshi, J. Am. Chem. Soc. 134 (2012) 15692.
[4] P. Pattanayak, J.L. Pratihar, D. Patra, A. Burrows, M. Mohan, S. Chattopadhyay, Eur. J. Inorg. Chem. (2007) 4263.
[5] P. Pattanayak, J.L. Pratihar, D. Patra, S. Mitra, A. Bhattacharyya, H.M. Lee, S. Chattopadhyay, Dalton Trans. (2009) 6220.
[6] P. Pattanayak, J.L. Pratihar, D. Patra, V.G. Puranik, S. Chattopadhyay, Polyhedron 27 (2008) 2209.
[7] P. Pattanayak, J.L. Pratihar, D. Patra, A. Burrows, M. Mohan, S. Chattopadhyay, Inorg. Chim. Acta 363 (2010) 2865.
[8] A. Basoglu, S. Parlayan, M. Ocak, H. Alp, H. Kantekin, M. Özdemir, Polyhedron 28 (2009) 1115.
[9] C.A. Langhoff, G.W. Robinson, Chem. Phys. 6 (1974) 34.
[10] J.S. Kim, D.T. Quang, Chem. Rev. 107 (2007) 3780.
[11] M. Calinescu, D. Manea, G. Pavelescu, Rev. Roum. Chim. 56 (2011) 231.
[12] C. Saudan, V. Balzani, P. Ceroni, M. Gorka, M. Maestri, V. Vicinelli, F. Vogtle, Tetrahedron 59 (2003) 3845.
[13] V. Pawlowski, H. Kunkely, A. Vogler, J. Photochem. Photobiol., A 161 (2004) 95.
[14] M. Osawa, M. Hoshino, D. Hashizume, Dalton Trans. (2008) 2248.
[15] R. Hou, T.-H. Huang, X.-J. Wang, X.-F. Jiang, Q.-L. Ni, L.-C. Gui, Y.-J. Fan, Y.L. Tan, Dalton Trans. 407 (2011) 551.
[16] A.I. Privalova, Ju.P. Morozova, E.R. Kashapova, V. Ja, J. Appl. Spectrosc. 78 (2011) 309.
[17] T.C. Chien, L.G. Dias, G.M. Arantes, L.G.C. Santos, E.R. Triboni, E.L. Bastos, M.J. Politi, J. Photochem. Photobiol., A 194 (2008) 37.
[18] L.M. Tolbert, S.M. Nesselroth, J. Phys. Chem. 25 (1991) 10331.
[19] A. McCarthy, A.A. Ruth, Phys. Chem. Chem. Phys. 13 (2011) 18661.
[20] P. Pattanayak, J.L. Pratihar, D. Patra, A. Burrows, M. Mohan, S. Chattopadhyay, J. Chem. Sci., in press.
[21] H. Warmke, W. Wiczk, T. Ossowski, Talanta 52 (2000) 449.
[22] N. Maiti, S. Pal, S. Chattopadhyay, Inorg. Chem. 40 (2001) 2204.
[23] D. Patra, J.L. Pratihar, B. Shee, P. Pattanayak, S. Chattopadhyay, Polyhedron 25 (2006) 2637.
[24] J.L. Pratihar, B. Shee, P. Pattanayak, D. Patra, A. Bhattacharyya, V.G. Puranik, C.H. Hung, S. Chattopadhyay, Eur. J. Inorg. Chem. (2007) 4272.
[25] J.L. Pratihar, N. Maiti, P. Pattanayak, S. Chattopadhyay, Polyhedron 24 (2005) 1953.
[26] T.B. Karpishin, T.D.P. Stack, K.N. Raymond, J. Am. Chem. Soc. 115 (1993) 182.
[27] T. Kawamoto, Y. Kushi, Bull. Chem. Soc. Jpn. 77 (2004) 289.
[28] T. Giaser, M. Heidemeier, T. Lügger, Dalton Trans. (2003) 2381.
[29] D.N. Neogi, A.N. Biswas, P. Das, R. Bhawmick, P. Bandyopadhyay, Inorg. Chim. Acta 360 (2007) 2181.
[30] S. Chattopadhyay, C. Sinha, P. Basu, A. Chakravorty, Organometallics 10 (1991) 1135.
[31] N. Maiti, B.K. Dirghangi, S. Chattopadhyay, Polyhedron 22 (2003) 109.
[32] G.M. Sheldrick, SHELXS-97, University of Göttingen, Göttingen, Germany, 1990.
[33] G.M. Sheldrick, SHELXL-97, Program for the Refinement of Crystals Structures from Diffraction Data, University of Göttingen, Göttingen, Germany, 1997.